Earth Syst. Dynam. Discuss., https://doi.org/10.5194/esd-2018-54
Manuscript under review for journal Earth Syst. Dynam.
Discussion started: 26 July 2018

Earth System Dynamics
Discussions
Open Access
EGU

Tracking the Choco jet since the 19th Century by using historical wind direction measurements

David Gallego[1], Ricardo García-Herrera[2,3], Francisco de Paula Gómez-Delgado[1], Paulina Ordoñez-Perez[4], Pedro Ribera[1]

[1]Departamento de Sistemas Físicos, Químicos y Naturales, Universidad Pablo de Olavide, Seville, 41013, Spain
[2]Departamento de Física de la Tierra y Astrofísica, Universidad Complutense, Madrid, 28040, Spain
[3]IGEO, Instituto de Geociencias (CSIC, UCM), Madrid, 28040, Spain
[4]Centro de Ciencias de la Atmósfera, Universidad Nacional Autónoma de México, Mexico City, 04510, Mexico

Correspondence to: David Gallego (dgalpuy@upo.es)

Abstract. In this paper, we demonstrate that the methodology recently developed to quantify the strength of monsoonal circulations by using historical wind direction observations can be applied to compute a new index for the intensity of the Choco jet. This is a low-level westerly jet observed from May to November whose core is located at 5º N and 80º W that modulates the moisture transport from the Pacific into Central America and northern South America. The Choco jet is profoundly related to the dynamics of the Intertropical Convergence Zone in the eastern equatorial Pacific and it is responsible of up to 30% of the total precipitation in these areas. We have been able to produce an index for this jet starting in the 19th century, adding almost a century of data to previous comparable indices. Our results indicate that the seasonal distribution of the precipitation in Central America has changed along the 20th century as a response to the changes in the Choco jet, with has diminished (increased) its strength in July (September). Additionally, we have found that the relation between the Choco jet and the El Niño / Southern Oscillation has been remarkably stable along the entire 20th century, a finding particularly significant because the stability of this relation is usually the basis of the hydrologic reconstructions in northern South America.

1 Introduction

The quantification of the moisture transport in the atmosphere requires a precise knowledge of the atmospheric motion (i.e. the wind field) and the three-dimensional distribution of water vapour (Gimeno, 2014). As global reanalysed datasets have become widely available and high resolution models have been applied to track the origin of atmospheric water (Sthol and James, 2004), a lot of research has addressed this topic. As a result, the recent variability of the moisture transport in the atmosphere is nowadays relatively well understood (Gimeno et al., 2012). Unfortunately, most of these works are limited to the second part of the 20th century (Marengo et al., 2004; Gimeno et al., 2012) or even to years after 1979, mainly because of the large uncertainties in the knowledge of the specific humidity before the satellite era, hampering the analysis of the long term moisture transport variability.

Earth Syst. Dynam. Discuss., https://doi.org/10.5194/esd-2018-54
Manuscript under review for journal Earth Syst. Dynam.
Discussion started: 26 July 2018

Earth System Dynamics Discussions

During the last years, it has been possible to assess the interannual variability of the moisture advected to landmasses by designing indices based solely on wind direction over some key areas (Garcia-Herrera et al., 2018 and references therein). The main advantage of these so-called "directional indices" is that by design, they only require the knowledge of the wind direction, a variable that has been routinely measured aboard sailing ships since the end of the 17th century. As a result of several data recovery projects (García-Herrera et al., 2005; Allan et al., 2011; Wilkinson et al., 2011 among others), millions of these early meteorological observations are nowadays incorporated into the International Comprehensive Ocean-Atmosphere Data Set (ICOADS) database (Freeman et al., 2016). In its most recent release ICOADS holds over 456 million individual marine reports, covering the period 1662-2014.

Directional indices have resulted excellent tools to quantify the moisture transport associated to monsoons because in these regions, the changes in precipitation are directly related to a seasonal wind reversal. Wind and precipitation changes are profoundly related and they are dynamically consistent through the "Gill pattern" (Gill, 1980), but they are not necessarily the same (Wang et al., 2014). Monsoonal areas based on wind changes are usually defined as those where the local summer westerly minus winter easterly at 850 hPa exceeds 50% of the annual mean zonal wind speed. The local summer/winter denotes May to September/November to March for the Northern Hemisphere and vice versa for the Southern Hemisphere (Wang et al., 2014). Figure 1.a shows the areas meeting this criterion based on zonal wind data from the NCEP/NCAR reanalysis data (Kalnay et al., 1996). In the case of precipitation, monsoonal areas are usually demarcated as those where the local summer minus winter precipitation rate exceeds 2 mm day^{-1}. Additionally, to distinguish between monsoon climate and arid/semiarid or Mediterranean climates and furthermore, to discriminate from equatorial perennial rainfall regimes, it is also required that the local summer precipitation exceeds 55% of the annual total areas (Conroy and Overpeck, 2011; Hsu et al., 2011; Wang et al., 2014). Figure 1.b shows these areas based on the CPC Merged Analysis of Precipitation (Xie and Arkin, 1997).

The intersection between the areas in Figs. 1.a and 1.b should be optimal for computing monsoonal directional indices based on wind changes highly representative of the moisture transport associated to a monsoon. However historical wind measurements were taken at the surface level, not at 850 hPa, and of course, they are only available along the ships' routes, so it is necessary to identify regions where the monsoonal wind reversal found at the 850 hPa level is also found at the surface. In this regard, Fig. 1.c shows the areas where local summer westerly minus winter easterly wind at the 0.995 sigma level exceeds 100% of the annual mean zonal wind speed. This is an analogous criterion as that used for the wind at 850 hPa but with a larger threshold in order to account for the greater wind variability at the near surface level. Additionally, Fig. 1.d shows the areas (in a 2.5º x 2.5º grid) where the last release of the ICOADS database currently has two or more wind direction observations per month for the summer months for at least 90 years in the 1900-2014 period. This is the minimum density of data considered necessary to build a meaningful directional index at monthly scale over the area typically used to

Earth Syst. Dynam. Discuss., https://doi.org/10.5194/esd-2018-54
Manuscript under review for journal Earth Syst. Dynam.
Discussion started: 26 July 2018

compute dynamical indices for a monsoon, spanning around 20º in longitude and 10º in latitude (Li and Zeng, 2002; Gallego et al., 2015).

The regions where the four previous conditions are simultaneously met are shown in Fig. 1.e and they can be considered as those where building dynamical indices for monsoon-like systems highly related to precipitation (based on historical data from ICOADS) is possible. Directional indices have already been developed for the obvious cases, i.e. the West African Monsoon (area centred at 8º N-20º W), the Indian Monsoon (15º N - 75º E), the Australian Summer Monsoon (10º S -120º E) or the Western North Pacific Summer Monsoon (15º N – 120º E) (Gallego et al., 2015; Ordoñez et al., 2016; Gallego et al., 2017; Vega et al., 2018 respectively). Interestingly, this general analysis identifies some other areas with monsoon-like behaviour in the Indian Ocean, north of Madagascar and a large area in the eastern tropical Pacific between 120º W and 80º W, extending between around 4º N and 15º N. Although both the wind and the precipitation in the latter region show a monsoon-like behaviour, this system is not a monsoon, but a low-level westerly jet known as the Choco jet. The name standing both as an acronym from "CHorro del Occidente COlombiano" (Western Colombian Jet) and as the place name "Chocó", one of the Colombia's regions most affected by this wind reversal. Between May and November, the winter wind regime characterized by predominant north-easterly winds in this part of the world is replaced by south westerlies at low levels. The consequent change in the moisture transport from the Pacific into the continent affects millions of people (Arias et al., 2015) and it has a profound impact on the western coast, from Costa Rica to northern Colombia, which, as a result, are among the rainiest places on earth (Poveda et al., 2014).

Quantifying the variability of this system is therefore of great importance and currently, the index used to measure the Choco jet strength is based on reanalysis products, limiting its availability to the second part of the 20th Century (Poveda and Mesa, 2000). Precipitation series in the area directly affected by the jet are also severely limited in time and they are not adequate to build longer indices (Carmona and Poveda, 2014). In view of the potential of this region evidenced by Fig. 1.e, we have developed a new directional index for the Choco jet. This adds almost a century to the current indices of this system.

2 The CHOCO-D index

A complete description of the concept of directional indices can be found in Barriopedro et al. (2014) and Gallego et al. (2015) and only a brief introduction is given here. These indices are based on daily observations of wind direction and are usually defined as the monthly frequency of wind direction coming from a given range of angles. Wind direction has been measured essentially in the same way since the early times of sailing, not needing any conversion beyond referring the observation to the geographic north. In fact, wind direction can be regarded as an instrumental measurement independently of the period and in consequence, directional indices can be considered instrumental ones.

Earth Syst. Dynam. Discuss., https://doi.org/10.5194/esd-2018-54
Manuscript under review for journal Earth Syst. Dynam.
Discussion started: 26 July 2018

Earth System Dynamics Discussions

For this work, raw wind direction measurements have been taken from the ICOADS database in its 3.0 release (Freeman et al., 2017). We selected the area [4º N-15º N ; 120º W-84º W] plus the area [4º N-9º N; 84º W-77.5º W], covering all of the outlined region over the eastern tropical Pacific in Fig. 1.e. Figure 2 shows the selected domain, while shading shows the 1800-2014 cumulative density of ICOADS observations in a 1ºx1º grid between May and November. The darkest gridpoints noticeable in the equatorial Pacific in Fig. 2 correspond to data taken by moored buoys, which in this region started in June 1986. Some of these buoys are inside the selected domain and due to their fixed location, far from the usual ship's routes, and their high temporal resolution, they became the dominant source of data since the 1990s in the selected domain. In order to maintain the homogeneity in the geographical distribution of the observed data into the domain, we did not consider data taken by moored buoys.

The graph at the bottom-left corner in Fig. 2 shows the resulting temporal evolution in the number of the available wind direction observations inside the selected area between May and November. Unfortunately, for the first half of the 19th Century ICOADS has a very poor coverage in the Pacific (typically below 100 observations between May and November). Around 1850 there is an increase in the data coverage and, for some years, up to around 1000 observations can be found. However, the number of observations diminishes again below 100 per year between 1860 and the final decade of the 19th Century. At the beginning of the 20th Century onwards, the number of observations is typically well over 1000 per year rising to more than 10000 after the final years of the 1950's decade. It is noteworthy that a large number of observations correspond to the routes following the coast, with a large contribution of the route from North America to the Panama Canal since its opening in the late 1910's. In fact, the latitude of the Panama Canal (around 9º N) was the southernmost latitude reached for most of the ships aimed to the Caribbean Sea.

Inside the selected area, we computed the so called CHOCO-D index (Choco - Directional index) as the percentage of days per month with prevalent wind flowing from the southwest (observed wind direction ranging between 180 to 270 degrees from the true north). Following the methodology of Barriopedro et al. (2014) we considered a day as "a day with prevalent wind flowing from the southwest" when at least 37% of the wind observations in the selected area for a given day reported this wind direction. This percentage was set as the one maximizing the average correlation between June and October for the 1948-2014 period with the NCEP/NCAR monthly zonal wind at 925 hPa averaged over the area [5º N-7.5 ºN; 90º W-80º W], which is considered a good representation of strength of the Choco jet core (Poveda and Mesa, 2000). It must be stressed that a sensitivity test (not shown) proves that the CHOCO-D index is scarcely sensitive to changes in the percentage used for its definition. A minimum of 10 days represented in a month was required to compute the index (Barriopedro et al., 2014).

The seasonal cycle of the NCEP-NCAR zonal wind at 925 hPa averaged over the area [5º N-7.5º N; 90º W-80º W] for the 1948 and 2014 period is displayed in Fig. 3.a (dashed blue line). As expected, the area is dominated by weak north easterly

winds between January and March, but this regime has already changed to a westward one by April and the westward component of the Choco jet is clearly evidenced between May and November by the positive values of the average zonal wind, which it is characterized by two relative maxima in June and October. The CHOCO-D index based exclusively on ICOADS wind direction observations (black line) closely mimics this seasonal march, with percentages of westerly days close to zero up to April, and higher values between May and November. Two relative maxima are found as well in June and September, a relative minimum is observed in July, coincident with the well-known midsummer drought in Central America (Small et al., 2007; Duran-Quesada et al., 2017). Figure 3.a also shows the monthly correlations between the averaged NCEP/NCAR zonal wind at 925 hPa and the CHOCO-D index for the concurrent 1948-2014 period. For all the active jet season, correlations are positive and significant, with a maximum value of +0.69 ($p<0.01$) for August and always above +0.50 ($p<0.01$) from May to October. With the exception of some years around 1960, the close agreement between the temporal series of the CHOCO-D index and the 925 hPa zonal wind for the (June-October average) is shown in Fig. 3.b. These values indicate that the CHOCO-D captures a significant part of the variability of the zonal winds at the core of the Choco jet.

As shown by Gallego et al. (2015), directional indices suffer from a certain uncertainty derived from the fact that the wind direction in the chosen sector is represented by a limited number of point observations. Consequently, it is related to the number of data used to compute the index. In this case, the region encompasses around 5,000,000 km^2. The inherent spatial variability of the wind inside this huge region and the finite number of available measurements in a given month is translated as dispersion in a particular realization of the index based on a finite sample of data. To estimate the expected uncertainty as a function of the number of available measurements, we computed 1000 'degraded' CHOCO-D indices constructed from N randomly selected wind observations inside the selected area with N ranging between 10 and 500. For each N, the 1000 degraded CHOCO-D are expected to be different because they are computed from a different set of observations. The average standard deviation of these 1000 series as a function of N between May and November is shown in Fig. 4 for the period 1971-2010. This particular period was selected in order to have a large-enough pool of wind observation in ICOADS to select a random sample of at least 500 observations. The results are scarcely dependent on the month and, as expected, the largest standard deviations are found for N=10 (around 16%) in all cases. This value rapidly decreases as N increases. For N=50 observations, the standard deviation is below 10% and, for N over 400, the standard deviation is almost stable around 6% to 7%. The fact that the standard deviation does not tend to cero as N increases reflects the inherent spatial variability of the wind inside the large region considered. We took the standard deviation shown in Fig. 4 as a conservative dispersion measure for the final CHOCO-D. It must be pointed out that this dispersion measure is purely empirical, depends on the region and it should be only interpreted as the expected standard deviation of a CHOCO-D value computed from a particular set of wind direction measurements and not as a confidence interval in a statistical sense.

Earth Syst. Dynam. Discuss., https://doi.org/10.5194/esd-2018-54
Manuscript under review for journal Earth Syst. Dynam.
Discussion started: 26 July 2018

3 Relation between the CHOCO-D and the moisture transport

Traditionally, it has been considered that the Caribbean Sea was the main moisture supplier for Central America and northern South America (Wang et al., 2006) through the Caribbean Low-Level Jet. However, the importance of the transport from the Pacific source by the Choco jet has been recently highlighted and it is estimated that the moisture advected from this ocean can contribute up to 30% of the total precipitation in areas of the western coast of Central America (Duran-Quesada et al., 2010; Duran-Quesada et al., 2017). The importance of the Pacific source is clearly evidenced in Fig. 5, which shows the difference between precipitation composites for months with CHOCO-D above and below one standard deviation of its average value for the 1901-2013 period ("positive" and "negative" Choco jet phases in successive) covered by the Global Precipitation Climatology Centre (v7) dataset (Becker et al., 2013). The precipitation changes associated to opposite anomalies of the CHOCO-D index extend over large areas of southern Mexico, Central America and spread southward into northern Colombia. The largest positive precipitation anomalies are found between July and September, when the Choco jet is fully developed, and they are especially noticeable in the western coast of Central America from Guatemala to Panama, where precipitation anomalies exceed 5 $mm \cdot day^{-1}$ during positive phases of the CHOCO-D in relation to the negative ones. The connection of these rainfall anomalies with the moisture advection has been assessed by computing the vertically integrated moisture transport through the 1000-700 hPa levels and the corresponding moisture convergence (Fig. 6). We limited the latter analysis to the 1979-2014 period because of the large uncertainties in the vertical distribution of the specific humidity in the NCEP/NCAR reanalysis over the equatorial Pacific prior to the satellite era. In order to attain a large enough number of cases for this shorter period, we relaxed the threshold for including positive/negative phases by considering the years above/below 0.75 standard deviation of the CHOCO-D index. Despite the different periods considered and the lower spatial resolution of the reanalysis, the agreement between Figs. 5 and 6 is remarkable. As expected, large CHOCO-D values appear related to an enhanced moisture transport (of up to 100 $kg \cdot m^{-1} \cdot s^{-1}$) from the Pacific into Central America in a latitude band extending from around 4º N to 15º N. The higher values of moisture convergence related to this enhanced transport are located over Panama and the pacific coast of Colombia, westward of the Cordillera Central. It is also interesting to note that the Pacific is a relevant moisture source for the Caribbean as well. Over this area, large values of moisture convergence occur, originating significant changes in the precipitation of the Greater Antilles, especially in Jamaica and large areas of Cuba (see Fig. 5.d for example).

4 Temporal evolution of the CHOCO-D index

4.1 Interannual and decadal variability

The exceptional time coverage of ICOADS allows building an almost continuous monthly record of the CHOCO-D index starting in the 1880s and for some years between 1850 and 1860 (Fig. 7). The series indicates that the Choco jet is rather

Earth Syst. Dynam. Discuss., https://doi.org/10.5194/esd-2018-54
Manuscript under review for journal Earth Syst. Dynam.
Discussion started: 26 July 2018

variable at interannual scale but the most prominent feature of the time evolution is a marked interdecadal variability, which is evident for all months (smoothed coloured curves in Fig. 7). This longer-term variability is quite dependent on the considered month. In general, the period 1880-1910 was characterized by stronger than average jets from May to August and also in November, while weaker than average jets are found in September and October. The subsequent three decades (1910-1940) show a general tendency to lower than average jets (except in November) which is quite evident in August. After the 1940s, the long term anomalies became even most dependent on the month. In May, the CHOCO-D shows an alternating behaviour at near decadal periods, while in June the index oscillates around average. In July and August the CHOCO-D was mostly below its low term average up to the 1990s, while in September and October it was above it up to the end of the series (2014), with a short period (1981-1990) of weak jets in October. November shows a long period of quite weak jets from 1960 to the late 1990s followed by a recovery to near-average values since the first years of the 21th century.

The strong dependence of the CHOCO-D behaviour on the month suggests that the seasonal distribution of the precipitation associated with the Pacific moisture source could be modulated by these long term changes in the Choco jet. Accounting for no more that 30% of the total precipitation in the area (Duran-Quesada et al., 2010), the changes in the total precipitation associated with the variability of the Choco jet are necessarily moderate, but yet discernible in cases of large opposite jet anomalies. For example, according to Fig. 7, the period 1901-1911 was characterized by a persistent strong jet in July and a relatively weak one in September. The contrary situation is observed in the 1965-1975, with a very weak jet in July and a strong one in September. When the GPCC difference in precipitation between the 11-year periods 1965-1975 and 1911-1901 is computed (Fig. 8), it is found that in July (September), the period 1965-1975 was significantly drier (wetter) than the 1911-1901 in large parts of Central America and northern Colombia, which changes in the total precipitation in the order of +/- 2 mm · day^{-1}.

4.2 Relation with ENSO

Ultimately the Choco jet originates in the southerly trade winds, making it strongly dependent on the meridional SST gradient along the Eastern Equatorial Pacific (Martinez et al., 2003). A diminished temperature gradient between the Peruvian Coast (El Niño 1+2 area) and the Panama Bight / northern Colombian western coast around 5º N during the developing phase of an El Niño event is accompanied by weaker trades and therefore, a weaker Choco jet (Poveda et al. 2001). In this way, a year with weak (strong) jet tends to be followed by El Niño (La Niña) conditions. The profound link between meridional SST gradient and the precipitation in western Colombia through the Choco jet has been documented for the second part of the 20th Century by Poveda and Mesa (2000) and Poveda et al. (2001) and it has been subsequently assumed as the basis for the reconstruction of the climate in the area since the last glaciation (Martinez et al., 2003). The long series of the CHOCO-D index allows to assess the stability of the relation between the Choco jet and the ENSO at secular scale for the first time. Figure 9 shows the correlation of the CHOCO-D index between July and September and the

Earth Syst. Dynam. Discuss., https://doi.org/10.5194/esd-2018-54
Manuscript under review for journal Earth Syst. Dynam.
Discussion started: 26 July 2018

following El Niño3.4 index (December to February of the following year) for variable timescale fluctuations in the absolute magnitude of the correlation are evident at short timescales, but for windows over 30 years, our results indicate that the correlation between the Choco jet and the ENSO has remained negative and relatively stable since the late years of the 19th century for the core of the jet season. This same result is found when the ENSO cycle is represented by the Southern Oscillation Index (Ropelewski and Jones, 1987) based on Sea Level Pressure instrumental measurements (not shown).

5 Discussion and conclusions

During the last years, a number of studies have dealt with climate reconstructions based on historical wind measurements (see Garcia-Herrera et al., 2018 for a recent review). However, due to the low number of historical meteorological records over the eastern Pacific, most of these works correspond to reconstructions over the North Atlantic or the Indian Oceans. The few exceptions considering the Pacific are limited to the study of the climatic implications in the changes in the duration of a particular shipping route (Garcia et al., 2001), focus on the westernmost Pacific (Vega et al., 2018) or have made use of indirect approaches, by estimating the climate in the tropical Pacific through the use present-time teleconnections patterns using data taken at other oceanic basins (e.g. Barrett et al., 2017a; Barrett et al., 2017b).

In this work, we have found that the strength of the Choco jet can be computed through a reliable index starting in the 1850's decade by using in-situ wind direction measurement contained in ICOADS and the methodologies recently developed to quantify monsoonal circulations. Up to our knowledge, this is the first time that it has been possible to construct a quantitative instrumental climate index over the eastern tropical Pacific for such a large period. This is because the exceptionally large latitude range where the monsoon-like changes in the wind direction can be related to the Choco jet. Although it had been widely shown in literature that the latitude of the Choco jet core is usually restricted to the 5º N-7º N range and it is maximum at 80ºW-90ºW (Poveda and Mesa, 2000; Sierra et al., 2017) we found that the optimal area for computing an index based solely on wind direction measurements at the surface level for this jet goes from 4º N to 15º N and extends from 120º W to 80º W. Over such a large area, the cumulative number of observations taken by ships, especially those sailing along the coast, resulted large enough to compute a meaningful index.

The reason beyond this fortunate circumstance is the profound link between the location of the Intertropical Convergence Zone (ITCZ) and the Choco jet (Waliser and Sommerville, 1994; Sierra et al., 2017). Forced by the north–south orientation of the South American coastland and the predominant position of the ITCZ north of the Equator between April and November, the southerly trade winds over the eastern Pacific cross the Equator acquiring a predominant westerly direction and entering the continent with maximum zonal velocity around the 5º N to 7º N latitude characteristic of the Choco jet core (Poveda and Mesa, 2000; Sakamoto et al., 2011; Arias et al., 2015). During the boreal winter, the southward migration of the ITCZ allows the north-easterly Northern Hemisphere trade winds to blow as southward as 4º N (Wodzicki and Rapp, 2016).

In this way, in this part of the world, the ITCZ separates the domain of winds with westward/eastward component always in the same hemisphere and its migration is the ultimate reason of the seasonal wind reversal observed in the tropical eastward Pacific and consequently its characterization as a "monsoonal" area by wind-based criteria (see Figs. 1.a and 1.c). Recently, Wodzicki and Rapp (2016) showed that the central latitude of the eastern Pacific ITCZ ranges between 4ºN and 10-12ºN. So, along the year, the ITCZ displaces between these limits, modifying the relation between the areas affected by winds with westward/eastward components and therefore the relative number of wind observations with wind blowing from the southwest inside the area where the CHOCO-D index is defined. This structure explains the excellent response of the CHOCO-D to the seasonal march of the Choco jet. Additionally, we also found that, even not including the wind velocity, the CHOCO-D is highly correlated with the indices currently used to measure this jet based on spatial averages of the zonal component of the wind.

As a consequence, the CHOCO-D is strongly representative of the moisture advection from the Pacific into Central America and northern South America and therefore, of a significant part of the precipitation in this area. We have found that since at least 1880, the Choco jet has experienced large changes at decadal scales. These are quite dependent on the month. Interestingly the July series shows a tendency to be above its long term average value from 1840 to 1910 and below this average from 1910 and 1990. September exhibits an opposite behaviour, being below average up to the 1920s and above it since that decade on. As the reversal in the trends for July and September occurred at the beginning of the 20th Century, the evaluation of the consequent changes in independent precipitation records are rather uncertain because of the low number of precipitation data in this part of the world during the first two decades of the 20th Century (Becker et al., 2013). Notwithstanding, the analysis of the GPCC dataset suggest that along the 20th century, there was a discernible change in the seasonal distribution of the precipitation related with the intra-annual variability of the Choco jet. Finally, it is worth mentioning that Carmona and Poveda (2014) found an increasing trend in the precipitation of the Pacific coast of Colombia starting in the last decades of the 20th century. Our results support this finding, as the strength of the Choco jet has been steadily increasing for May, June, July and August since the last years of the 20th century (Fig. 7

Finally, since their conception, one of the main applications of directional indices has been the analysis of the stability of teleconnection patterns. For instance, directional indices have been used to prove that the relation between the strength of the West African monsoon and the ENSO or the Atlantic Multidecadal Oscillation have been quite unstable (Gallego et al., 2015). Similarly, instabilities have been described in the relation between the ENSO and the strength of the Western North Pacific Summer monsoon (Vega et al., 2018). On the contrary, we have found than the relation between the Choco jet strength and the ENSO has been remarkably stable at least since the 1880s. This is particularly relevant because the stability of this relation is usually the basis of the hydrologic reconstruction or prediction in northern South America (Gutiérrez and Dracup, 2001; Prange et al., 2010; Córdoba-Machado et al., 2015).

Acknowledgements

This research was funded by the Spanish Ministerio de Economía y Competitividad through the projects CGL2013-44530-P, CGL2014-51721-REDT and the research group RNM-356 belonging to the "Plan Andaluz de Investigación Desarrollo e Innovación". NCEP Reanalysis Derived data, CMAP Precipitation data and GPCC Precipitation data provided by the NOAA/OAR/ESRL PSD, Boulder, Colorado, USA, from their Web site at http://www.esrl.noaa.gov/psd/. ICOADS data provided by the NCAR/UCAR Research Data Archive, from their Web site at https://rda.ucar.edu/datasets/ds548.0/.

References

Allan, R., Brohan, P., Compo, G. P., Stone, R., Luterbacher, J., and Brönnimann, S.: The International Atmospheric Circulation Reconstructions over the Earth (ACRE) Initiative, Bull. Amer. Meteor. Soc., 92, 1421–1425, doi:10.1175/2011BAMS3218.1, 2011.

Arias P. A., Martínez, J. A., and Vieira, S. C.: Moisture sources to the 2010–2012 anomalous wet season in northern South America, Clim. Dynam., 45, 2861–2884, doi:https://doi.org/10.1007/s00382-015-2511-7, 2015.

Barrett, H. G., Jones, J. M., and Bigg, G. R.: Reconstructing El Niño Southern Oscillation using data from ships' logbooks, 1815–1854. Part I: methodology and evaluation, Clim. Dynam., 50, 845–862, doi:https://doi.org/10.1007/s00382-017-3644-7, 2017a.

Barrett, H. G., Jones, J. M., and Bigg, G. R.: Reconstructing El Niño Southern Oscillation using data from ships' logbooks, 1815–1854. Part II: Comparisons with existing ENSO reconstructions and implications for reconstructing ENSO diversity, Clim. Dynam., 50, 3131–3152, doi:https://doi.org/10.1007/s00382-017-3797-4, 2017b.

Barriopedro, D., Gallego, D., Alvarez-Castro, M. C., Garcia-Herrera, R., Wheeler, D., Peña-Ortiz, C., and Barbosa, S. M.: Witnessing North Atlantic westerlies variability from ship's logbooks (1685-2008), Clim. Dynam., 43, 939–955. doi:10.1007/s00382-013-1957-8, 2014.

Becker, A., Finger, P., Meyer-Christoffer, A., Rudolf, B., Schamm, K., Schneider, U., and Ziese, M.: A description of the global land-surface precipitation data products of the Global Precipitation Climatology Centre with sample applications including centennial (trend) analysis from 1901–present, Earth Syst. Sci. Data, 5, 71-99, doi:10.5194/essd-5-71-2013, 2013.

Carmona A. and Poveda G.: Detection of long-term trends in monthly hydro-climatic series of Colombia through Empirical Mode Decomposition, Climatic Change, 123, 301-313, doi:10.1007/s10584-013-1046-3, 2014.

Cleveland W. S.: Robust locally weighted regression and smoothing scatterplots. J. Am. Stat. Assoc, 74, 829-836, doi:10.1080/01621459.1979.10481038, 1979.

Conroy, J. L. and Overpeck, J. T.: Regionalization of present-day precipitation in the greater monsoon region of Asia, J. Climate, 24, 4073–4095, doi: https://doi.org/10.1175/2011JCLI4033.1, 2011.

Córdoba-Machado, S., Palomino-Lemus, R., Gámiz-Fortis, S. R., Castro-Díez, Y., and Esteban-Parra, M. J.: Influence of tropical Pacific SST on seasonal precipitation in Colombia: prediction using El Niño and El Niño Modoki, Clim. Dynam., 44, 1293–1310, doi:https://doi.org/10.1007/s00382-014-2232-3, 2015.

Durán-Quesada, A. M., Gimeno, L., Amador, J. A., and Nieto, R.: Moisture sources for Central America: Identification of moisture sources using a Lagrangian analysis technique, J. Geophys. Res., 115, D05103, doi: 10.1029/2009JD012455, 2010.

Durán-Quesada, A. M., Gimeno, L., and Amador, J.: Role of moisture transport for Central American precipitation, Earth Syst. Dynam., 8, 147-161, doi: https://doi.org/10.5194/esd-8-147-2017, 2017.

Freeman, E., Woodruff, S. D., Worley, S. J., Lubker, S. J., Kent, E. C., Angel, W. E., Berry, D. I., Brohan, P., Eastman, R., Gates, L., Gloeden, W., Ji, Z., Lawrimore, J., Rayner, N. A., Rosenhagen, G., and Smith, S. R.: ICOADS Release 3.0: A major update to the historical marine climate record. Int. J. Climatol. (CLIMAR-IV Special Issue), 37, 2211-2237, doi:10.1002/joc.4775, 2017.

Gallego, D., Ordóñez, P., Ribera, P., Peña-Ortiz, C., and García-Herrera, R.: An instrumental index of the West African Monsoon back to the 19th century, Q. J. Roy. Meteor. Soc., 141, 3166-3176, doi: 10.1002/qj.2601, 2015.

Gallego, D., García-Herrera, R., Peña-Ortiz, C., and Ribera, P.: The steady increase of the Australian Summer Monsoon in the last 200 years. Sci. Rep-UK, 7, Article number: 16166, doi: 10.1038/s41598-017-16414-1, 2017.

Garcia, R. R., Díaz, H. F., García-Herrera, R., Eischeid, J., Prieto, M. R., Hernández, E., Gimeno, L., Durán, F. R., and Bascary, A. M.: Atmospheric Circulation Changes in the Tropical Pacific Inferred from the Voyages of the Manila Galleons in the Sixteenth–Eighteenth Centuries, Bull. Amer. Meteor. Soc., 82, 2435–2456, doi:https://doi.org/10.1175/1520-0477(2001)082<2435:ACCITT>2.3.CO;2, 2001.

García-Herrera, R., Können, G. P., Wheeler, D. A., Prieto, M. R., Jones, P. D., and Koek F. B.: CLIWOC: a climatological database for the World's Oceans 1750–1854, Climatic Change, 73, 1–12, doi:10.1007/s10584-005-6952-6, 2005.

Garcia-Herrera, R., Barriopedro, D., Gallego, D., Mellado-Cano, J., Wheeler, D., Wilkinson, C.: Understanding weather and climate of the last 300 years from ship's logbooks, WIREs Clim. Change, e544, doi:10.1002/wcc.544, 2018.

Gill, A. E.: Some simple solutions for heat-induced tropical circulation. Q. J. Roy. Meteor. Soc., 106, 447–462, doi:10.1002/qj.49710644905, 1980.

Gimeno, L., Stohl, A., Trigo, R. M., Dominguez, F., Yoshimura, K., Yu, L., Drumond, A., Durán-Quesada, A. M., and Nieto R.: Oceanic and terrestrial sources of continental precipitation, Rev. Geophys., 50, RG4003, doi:10.1029/2012RG000389, 2012.

Gimeno, L.: Oceanic sources of continental precipitation, Water Resour. Res., 50, 3647–3649, doi:10.1002/2014WR015477, 2014.

Gutiérrez, F. and Dracup, J. A.: An analysis of the feasibility of long-range streamflow forecasting for Colombia using El Niño–Southern Oscillation indicators, J. Hydrol., 246, 181-196, doi:https://doi.org/10.1016/S0022-1694(01)00373-0, 2001.

Hsu, P. C., Li, T., and Wang, B.: Trends in global monsoon area and precipitation over the past 30 years, Geophys. Res. Lett., 38, L08701, doi:10.1029/2011GL046893, 2011.

Kalnay, E., Kanamitsu, M., Kistler, R., Collins, W., Deaven, D., Gandin, L., Iredell, M., Saha, S., White, G., Woollen, J., Zhu, Y., Leetmaa, A., Reynolds, R., Chelliah, M., Ebisuzaki, W., Higgins, W., Janowiak, J., Mo, K. C., Ropelewski, C., Wang, J., Jenne, R., and Joseph, D.: The NCEP/NCAR 40-Year Reanalysis Project, Bull. Amer. Meteor. Soc., 77, 437–471, doi: 10.1175/1520-0477(1996)077<0437:TNYRP>2.0.CO;2., 1996.

Li, J. and Zeng, Q.: A unified monsoon index, Geophys. Res. Lett., 29, 1274, doi:10.1029/2001GL013874, 2002.

Marengo, J. A., Soares, W. R. Saulo, C., and Nicolini, M.: Climatology of the Low-Level Jet East of the Andes as Derived from the NCEP–NCAR Reanalyses: Characteristics and Temporal Variability, J. Climate, 17, 2261–2280, doi:https://doi.org/10.1175/1520-0442(2004)017<2261:COTLJE>2.0.CO;2, 2004.

Martínez, I., Keigwin, L., Barrows, T. T., Yokoyama, Y., and Southon, J.: La Niña-like conditions in the eastern equatorial Pacific and a stronger Choco jet in the northern Andes during the last glaciation, Paleoceanography, 18, 1033, doi:10.1029/2002PA000877, 2, 2003

Ordóñez P, Gallego, D., Ribera, P., Peña-Ortiz, C., and García-Herrera, R.: Tracking the Indian Summer Monsoon onset back to the pre-instrumental period, J. Climate, 29, 8115-8127, doi:10.1175/JCLI-D-15-0788.1, 2016.

Poveda G. and Mesa O. J.: On the existence of Lloró (the rainiest locality on Earth): Enhanced ocean-land-atmosphere interaction by a low-level jet. Geophys. Res. Lett., 27, 1675-1678, doi:https://doi.org/10.1029/1999GL006091, 2000.

Poveda, G., Jaramillo, A., Gil, M. M., Quiceno, N., and Mantilla, R. I.: Seasonally in ENSO-related precipitation, river discharges, soil moisture, and vegetation index in Colombia, Water Resour. Res., 37, 2169–2178, doi:10.1029/2000WR900395. 2001.

Poveda, G., Jaramillo, L., and Vallejo, L. F.: Seasonal precipitation patterns along pathways of South American low-level jets and aerial rivers, Water Resour. Res., 50, 98–118, doi:10.1002/2013WR014087, 2014.

Prange, M., Steph, S.; Schulz, M., Keigwin, L. D.: Inferring moisture transport across Central America: Can modern analogs of climate variability help reconcile paleosalinity records?, Quaternary Sci. Rev., 29, 1317-1321, doi:https://doi.org/10.1016/j.quascirev.2010.02.029, 2010.

Ropelewski, C. F. and Jones, P. D.: An extension of the Tahiti-Darwin Southern Oscillation Index. Mon. Weather Rev., 115, 2161-2165, doi:https://doi.org/10.1175/1520-0493(1987)115<2161:AEOTTS>2.0.CO;2, 1987.

Sakamoto M. S., Ambrizzi, T. and, Poveda, G.: Moisture sources and life cycle of convective systems over Western Colombia, Adv. Meteorol., Article ID 890759, 11 pages, doi:https://doi.org/10.1155/2011/890759, 2011.

Sierra, J. P., Arias, P. A., Vieira, S. C., and Agudelo, J.: How well do CMIP5 models simulate the low-level jet in western Colombia?, Clim Dynam., first online, https://doi.org/10.1007/s00382-017-4010-5, 2017.

Small, R.J., de Szoeke, S.P., and Xie, S.: The Central American Midsummer Drought: Regional Aspects and Large-Scale Forcing, J. Climate, 20, 4853–4873, doi:https://doi.org/10.1175/JCLI4261.1, 2007.

Stohl, A. and James, P.: A Lagrangian analysis of the atmospheric branch of the global water cycle. Part I: Method description, validation, and demonstration for the August 2002 flooding in central Europe, J. Hydrometeorol., 5, 656–678, doi:10.1175/1525-7541(2004)005<0656:ALAOTA>2.0.CO;2, 2004.

Vega I., Gallego D., Ribera P., Gómez-Delgado FdP., García-Herrera R., and Peña-Ortiz C.: Reconstructing the Western North Pacific Summer Monsoon since the late 19th century, J. Climate, 31, 355-368, doi:10.1175/JCLI-D-17-0336.1, 2018.

Waliser, D. E. and Somerville, R. C.: Preferred Latitudes of the Intertropical Convergence Zone. J. Atmos. Sci., 51, 1619–1639, doi:https://doi.org/10.1175/1520-0469(1994)051<1619:PLOTIC>2.0.CO;2, 1994.

Wang, C., Enfield, D. B., Lee, S., and Landsea, C. W.: Influences of the Atlantic Warm Pool on Western Hemisphere Summer Rainfall and Atlantic Hurricanes, J. Climate, 19, 3011–3028, doi:https://doi.org/10.1175/JCLI3770.1, 2006.

Wang, P. X., Wang, B., Cheng, H., Fasullo, J., Guo, Z. T., Kiefer, T., and Liu, Z. Y.: The global monsoon across timescales: coherent variability of regional monsoons, Clim. Past, 10, 2007-2052, doi:10.5194/cp-10-2007-2014, 2014.

Wilkinson, C., Woodruff, S. D., Brohan, P., Claesson, S., Freeman, E., Koek, F., Lubker, S. J., Marzin, C., and Wheeler, D.: Recovery of logbooks and international marine data: the RECLAIM project, Int. J. Climatol., 31, 968–979. doi:10.1002/joc.2102, 2011.

Wodzicki, K. R. and Rapp, A. D.: Long-term characterization of the Pacific ITCZ using TRMM, GPCP, and ERA-Interim, J. Geophys. Res. Atmos., 121, 3153–3170, doi:10.1002/2015JD024458, 2016.

Xie, P. and Arkin, P.A.: Global precipitation: A 17-year monthly analysis based on gauge observations, satellite estimates, and numerical model outputs. Bull. Amer. Meteor. Soc., 78, 2539–2558, doi:https://doi.org/10.1175/1520-0477(1997)078<2539:GPAYMA>2.0.CO;2, 1997.

Earth Syst. Dynam. Discuss., https://doi.org/10.5194/esd-2018-54
Manuscript under review for journal Earth Syst. Dynam.
Discussion started: 26 July 2018

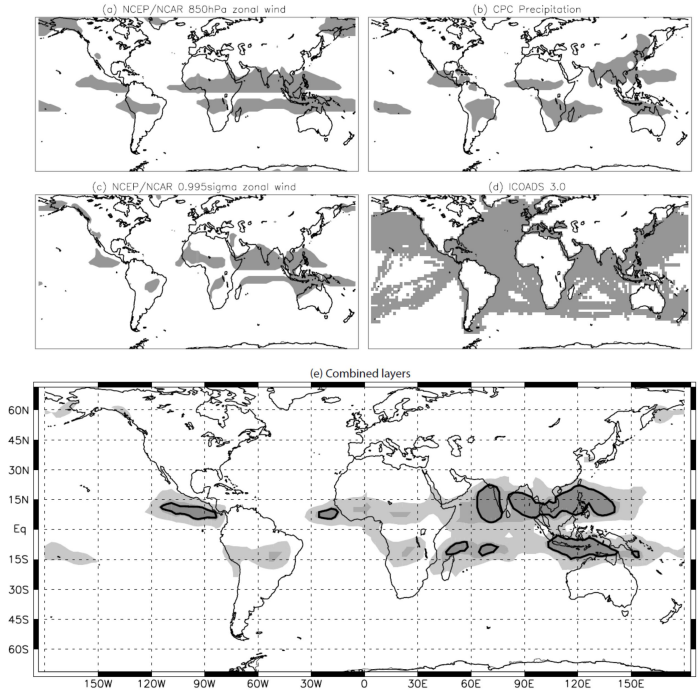

Figure 1: (a) Monsoonal areas according with a wind criteria at 850 hPa, (b) monsoonal areas according with a precipitation criteria, (c) Monsoonal areas according with a wind criteria at the near surface level, (d) Areas in which the ICOADS database has adequate coverage to build a directional index since 1900 and (e) Areas where two or more (light grey), three or more (darker grey) and all four (darkest grey and outlined) of the criteria selected do define a monsoonal area feasible to be quantified using ICOADS data are simultaneously met.

Earth Syst. Dynam. Discuss., https://doi.org/10.5194/esd-2018-54
Manuscript under review for journal Earth Syst. Dynam.
Discussion started: 26 July 2018

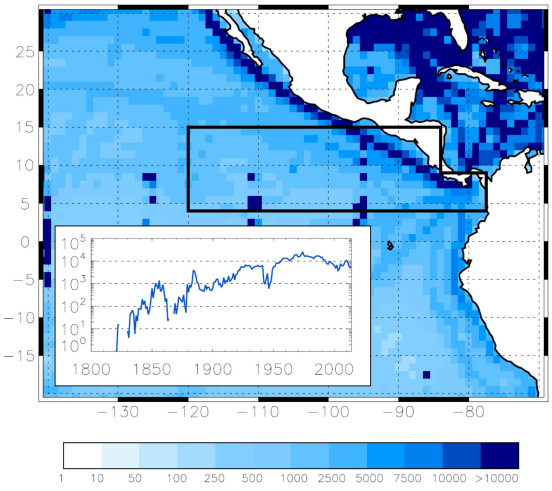

Figure 2: Number of wind direction observations in a 1x1 grid (May to November) and the 1800-2014 period available in ICOADS 3.0. Black contour indicates the area selected to compute the CHOCO-D index [4ºN-15ºN ; 120ºW-80ºW]. The graph at the bottom-left shows the time evolution of the cumulative number of wind direction observations inside the selected domain not considering data taken at moored buoys (note the logarithmic y-scale).

Earth Syst. Dynam. Discuss., https://doi.org/10.5194/esd-2018-54
Manuscript under review for journal Earth Syst. Dynam.
Discussion started: 26 July 2018

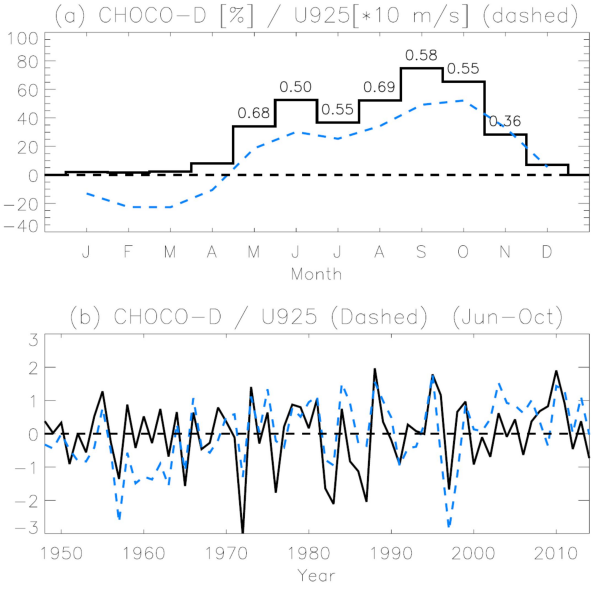

Figure 3: (a) Monthly averages (1948-2014) of the NCEP-NCAR zonal wind at 925 hPa averaged over the [5º N-7.5º N; 90º W-80º W] area (blue dashed line) and monthly averages of the CHOCO-D index for the same period in % of days in a month with prevailing wind flowing from the southwest (black line). Numbers over the CHOCO-D values indicates the monthly correlation between both series for the 1948-2014 period. Only correlations statistically significant (p<0.01) are displayed. Note the scale of the wind is expressed as 10 * m·s^{-1} to ease comparison. (b) Standardized temporal series (June to October average) of the CHOCO-D index and the NCEP-NCAR zonal wind at 925 hPa averaged over the [5º N-7.5º N; 90º W-80º W] (blue dashed line).

Earth Syst. Dynam. Discuss., https://doi.org/10.5194/esd-2018-54
Manuscript under review for journal Earth Syst. Dynam.
Discussion started: 26 July 2018

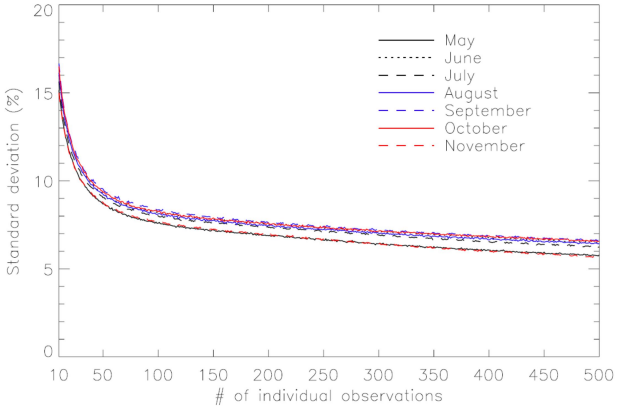

Figure 4: Expected dispersion (in %) of the CHOCO-D as a function of the number of wind direction observations used to compute it (x-axis) for May to November.

Earth Syst. Dynam. Discuss., https://doi.org/10.5194/esd-2018-54
Manuscript under review for journal Earth Syst. Dynam.
Discussion started: 26 July 2018

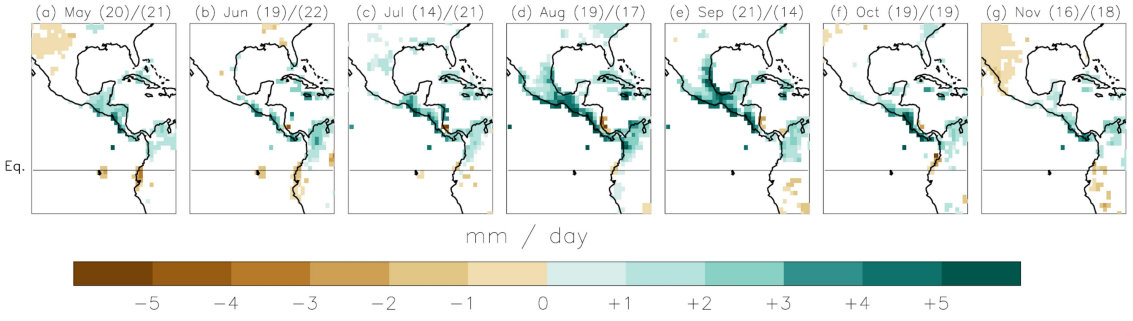

Figure 5: GPCC Precipitation differences between months with CHOCO-D over +/- 1 standard deviation for the 1901-2013 period (number of +1/-1 cases are indicated in brackets). Only areas with precipitation differences statistically significant at p<0.05 are represented.

Earth Syst. Dynam. Discuss., https://doi.org/10.5194/esd-2018-54
Manuscript under review for journal Earth Syst. Dynam.
Discussion started: 26 July 2018

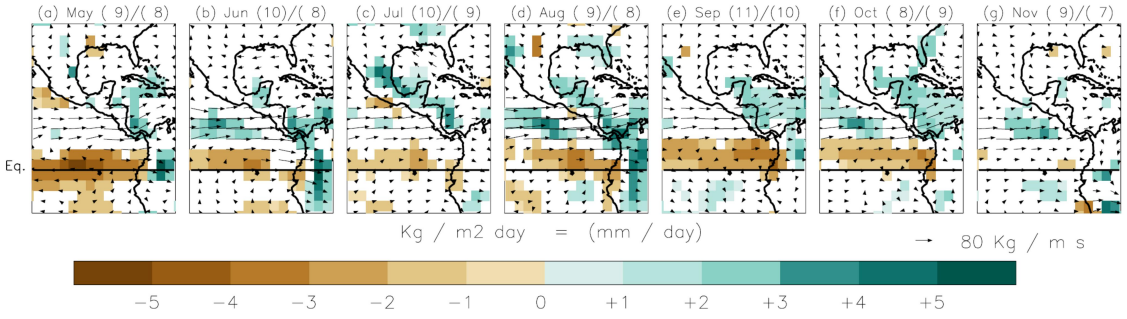

Figure 6: 1000-700 hPa vertically integrated moisture transport (arrows, scale at the lower-right corner) and moisture convergence (shaded areas) differences between CHOCO-D +/- 0.75 standard deviations years for the 1979-2014 period and NCEP/NCAR reanalysis data. Only moisture convergence differences significant at p<0.05 are represented. The number of CHOCO-D positive/negative cases used to compute the anomalies are indicated in brackets.

Earth Syst. Dynam. Discuss., https://doi.org/10.5194/esd-2018-54
Manuscript under review for journal Earth Syst. Dynam.
Discussion started: 26 July 2018

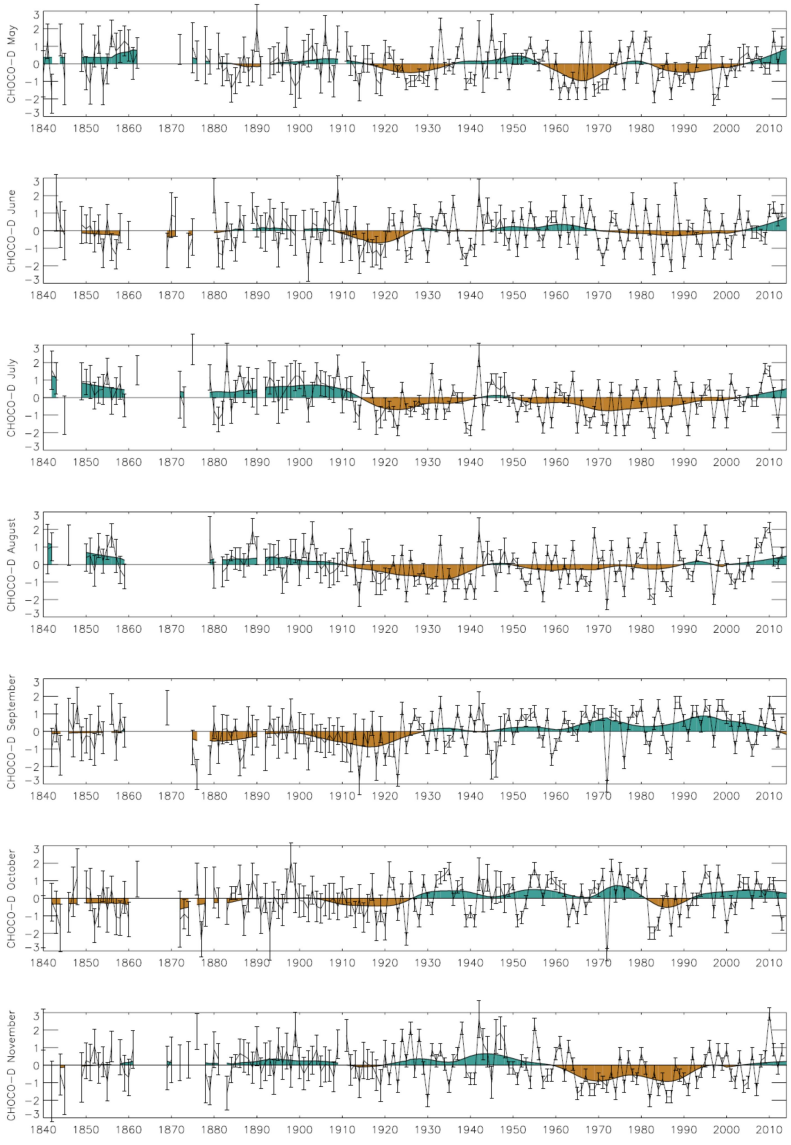

Figure 7: Standardized CHOCO-D for May to November between 1840 and 2014. Error bars indicate the expected standard deviation based on the number of observations available each year in ICOADS 3.0 (see text for details). Shaded smoothed curve is computed as a robust locally weighted regression with a 31-year window (Cleveland, 1979).

Earth Syst. Dynam. Discuss., https://doi.org/10.5194/esd-2018-54
Manuscript under review for journal Earth Syst. Dynam.
Discussion started: 26 July 2018

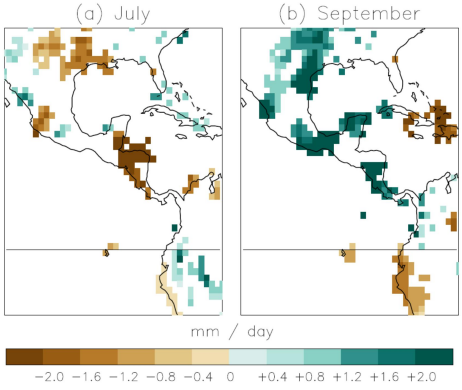

Figure 8: GPCC precipitation differences between the 11-year period 1965-1975 and 1901-1911 for a) July and b) September. Only differences at p<0.05 are displayed.

Earth Syst. Dynam. Discuss., https://doi.org/10.5194/esd-2018-54
Manuscript under review for journal Earth Syst. Dynam.
Discussion started: 26 July 2018

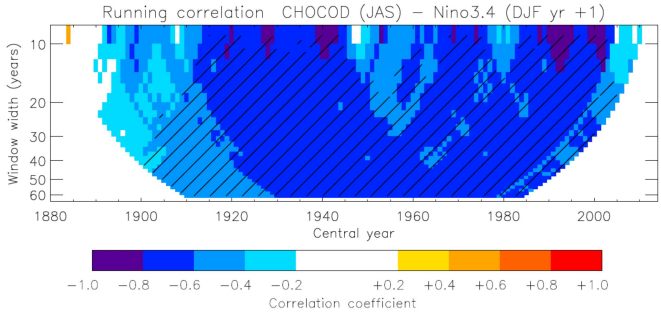

Figure 9: Running Pearson's correlation coefficient for variable window width (y-axis) between the July-August-September average CHOCO-D and the El Niño3.4 index averaged for December-January(year+1)-February(year+1). Hatched areas indicates statistically significant correlation at p<0.05.